Chemical Science

ROYAL SOCIETY OF CHEMISTRY

EDGE ARTICLE

View Article Online
View Journal | View Issue

Cite this: *Chem. Sci.*, 2026, **17**, 6939

All publication charges for this article have been paid for by the Royal Society of Chemistry

Received 30th October 2025
Accepted 4th February 2026

DOI: 10.1039/d5sc08385k

rsc.li/chemical-science

A new class of customisable stable boronic ester assemblies

D. Coomber, [a] O. Rusli, [b] H. Sharma,[a] H. E. Lee,[b] J. D. Evans, [c] N. J. Rijs, [b] C. Hua [d] and F. Pfeffer *[a]

An efficient, customisable approach for the assembly of covalent macrocycles and cages has been developed using the reaction of fused polynorbornane based bis-diols and commercially available boronic acids. The ability to customise the requisite bis-diol to various lengths and dihedral angles (here both 90° and 180°) and then combine with di or triboronic acids allows access to range of architectures. The resultant constructs were resistant to hydrolysis including 24-hour exposure to dilute solutions of either acetic or trifluoroacetic acid.

1. Introduction

Dynamic covalent chemistry (DCC) is a powerful method for accessing molecular architectures (including macrocycles, molecular cages, and covalent organic frameworks) under thermodynamic control. While several dynamic reactions have been employed to date[1–7] the use of boronic esters has generated several remarkable assemblies, such as the [12 + 8] molecular cages from both Mastalerz[8] and Beuerle[9] that boast exceptionally high porosities (>3000 g per m^2 BET), and the [2 + 2] macrocycles from Ono and Iwasawa[10,11] that act as supramolecular catalysts.

As boronic ester formation is a condensation reaction, many architectures are prone to complete disassembly in the presence of water or methanol (see Northrop[12,13] or Akine[14]). A landmark approach for improving stability was recently described by Kirchner and Beuerle,[15] whereby incorporating steric bulk (*t*-Bu groups) around the phenyl diboronic acid tecton **2** conferred stability to the final [12 + 8] 'cube' (Fig. 1). Notably, the cube was stable in (1 : 1) chloroform/methanol solution—even in the presence of acetic acid—with trifluoroacetic acid required for disassembly. The strategy, while effective, necessitated multistep synthesis of a custom boronic acid tecton. This effort was in addition to that required for synthesis of the tris-catechol tecton **1** (Fig. 1).

A surprisingly underexplored strategy for improving stability is variation of the diol component of the tecton—the vast majority of examples are based on catechol (see Northrop,[12,13,16,17] Kobayashi,[18] Akine,[14] Mastalarz[8,19] and Beuerle[20,21]). Indeed, outside of the library of cyclopentanediol examples from Iwasawa[22,23] and the recent bicyclo[2.2.2]octane diol example from Yamada,[24] few examples exist in which aliphatic diols are employed. Of considerable interest, simple aliphatic diols have been shown to form hydrolytically stable boronic esters,[25] and Roy and Brown specifically identified *exo*-norbornane diols as forming thermodynamically stable boronic esters—more stable than both catechol based and cyclopentanediol based boronic esters.[26,27]† It is therefore surprising that the use of tectons based on norbornane diols in the assembly of robust architectures has yet to be explored.

It was envisaged that *exo*-norbornane diols could be incorporated as terminal units in a fused [n]polynorbornane scaffold (Fig. 1) and these tectons would ultimately generate highly stable boronic ester assemblies upon reaction with readily available boronic acids. The known, efficient, convergent methodology[28–33] to access fused [*n*]polynorbornane frameworks of predictable, conformationally preorganised geometries made this an attractive proposition as related frameworks have been used in anion recognition[34–36] as well as the assembly of metal organic cages[37,38] and metal organic frameworks.[39]

Herein, the synthesis of two bis(norbornane diol) tectons and their self-assembly into macrocycles and molecular cages has been completed with absolute structures determined by single crystal X-ray diffraction (SC-XRD). Furthermore, the stability of the norbornane boronic ester assemblies to acid catalysed hydrolysis (both AcOH and TFA) has also been established.

2. Results and discussion

2.1 Synthesis of tectons

Two separate bis-diol tectons **3** and **4** were devised featuring different lengths and with dihedral angles of 90° and 180° respectively (Fig. 1). The angles were selected such that upon reaction with commercially available symmetric, planar di- and

[a]*School of Life and Environmental Sciences, Centre for Sustainable Bioproducts, Deakin University, Waurn Ponds, VIC 3216, Australia. E-mail: fred.pfeffer@deakin.edu.au*

[b]*School of Chemistry, University of New South Wales, Sydney, NSW 2052, Australia*

[c]*School of Physics, Chemistry and Earth Sciences, Adelaide University, Adelaide, SA 5005, Australia*

[d]*School of Chemistry, The University of Melbourne, Parkville, VIC 3010, Australia*

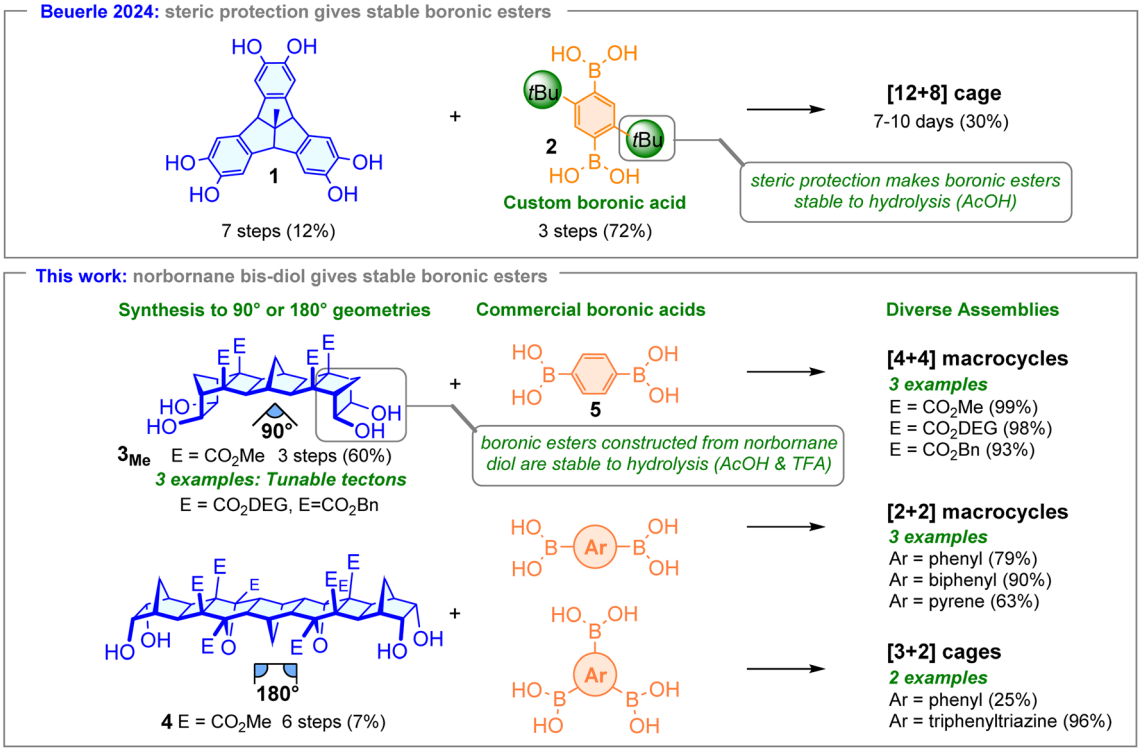

Fig. 1 Approaches to stable boronic ester architectures.

tri-boronic acids both macrocycles and cages could be constructed.

For the shorter tecton featuring a 90° dihedral angle, synthesis was accomplished in only three steps from readily available materials (Scheme 1). The ruthenium catalysed Mitsudo reaction of norbornadiene **6** with dimethyl acetylenedicarboxylate (DMAD) afforded tetraester $\mathbf{7_{Me}}$,[40] and subsequent Diels–Alder cycloaddition with cyclopentadiene (CPD) gave diene $\mathbf{8_{Me}}$. Upjohn dihydroxylation afforded the desired bis-diol $\mathbf{3_{Me}}$ in excellent 98% yield (60% overall/3 steps). The overall structure of the bis-diol was confirmed by SC-XRD and found to have a dihedral angle ~95° (see SI for full details). An advantage of the approach was compatibility with Upjohn dihydroxylation. For related aliphatic bis-diol tectons synthesised by Iwasawa[22] and Yamada,[24] the Upjohn dihydroxylation of bis(cyclopentene) or bis(bicyclo[2.2.2]octene) scaffolds was not stereoselective and as such only modest yields (35% and 27% respectively) of the desired tectons were obtained. For the norbornane based scaffold $\mathbf{8_{Me}}$ the Upjohn dihydroxylation was completely

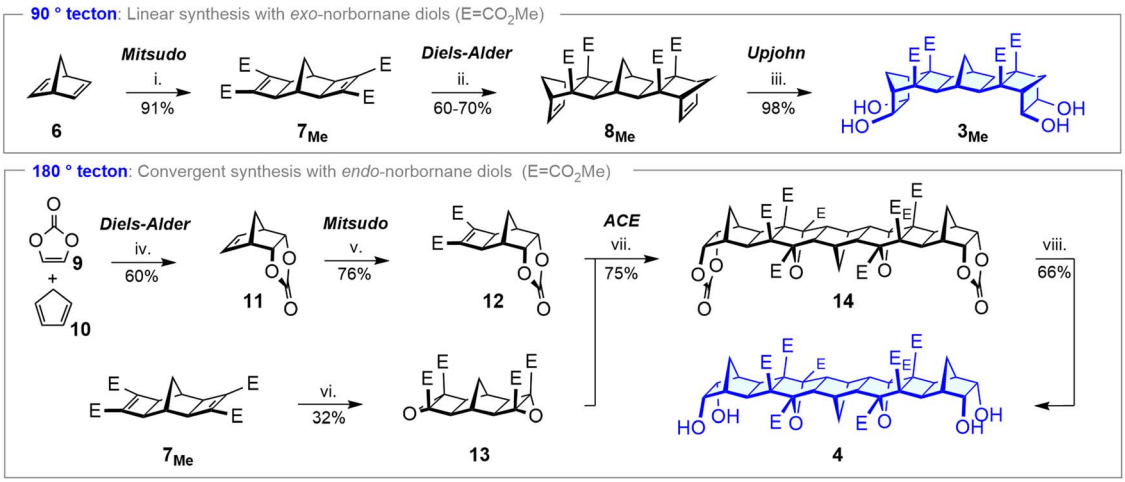

Scheme 1 Synthesis of 90° tecton $\mathbf{3_{Me}}$. (i) DMAD (2.2 eq.), $RuH_2(CO)(PPh_3)_3$ (4 mol%), DMF, 100 °C, 24 h. (ii) CPD (8 eq.), DMF, RT, 7 days. (iii) OsO_4 (1 mol%), NMO (3.6 eq.), acetone : H_2O (7 : 1), RT, 3 days. Synthesis of 180° tecton **4**. (iv). DMF, 150 °C, 75 min, μw. (v) DMAD (1.5 eq.), $RuH_2(CO)(PPh_3)_3$ (2.5 mol%), acetone, 100 °C, 60 minutes, μw. (vi) *t*-BuOOH (2.5 eq.), *t*-BuOK (0.5 eq.), THF, RT, 12 h. (vii) THF, 150 °C, μw. (viii) MeOH : H_2O (9 : 1), Cs_2CO_3 (3 eq.), reflux, 2 h.

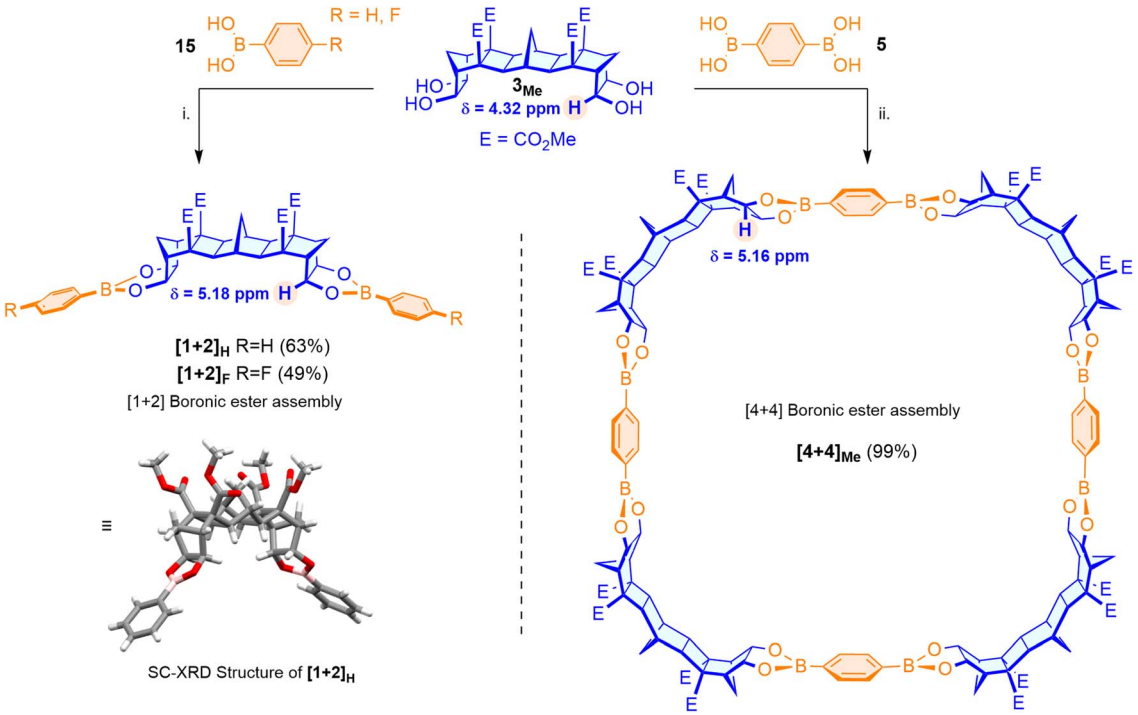

Scheme 2 Synthesis of [1 + 2] assemblies and [4 + 4] macrocycle. (i) EtOH, 130 °C, 5 min, μw. (ii) $CHCl_3$, 100 °C, 12 h.

stereoselective for *exo*-addition, and highly efficient (yields consistently >90%).

For tecton **4** featuring a 180° dihedral angle, the use of terminal *endo*-norbornane diol groups was envisaged (Fig. 1 and Scheme 1). First, the known *endo*-carbonate **11** was synthesised using a method adapted from Nencka *et al.*[41] before Mitsudo reaction[42] was used to access diester carbonate **12**. Microwave mediated 1,3-dipolar ACE cycloaddition of the carbonate **12** with the known bis-epoxide **13**[29] furnished the fused [5]poly-norbornane bis-carbonate framework **14**. Following decarboxylation, the desired bis-diol tecton **4** was isolated in 66% yield (7% overall/6 steps).

The two methods highlight the versatility of the poly-norbornane approach, employing multiple, stereoselective cycloadditions (Mitsudo, Diels–Alder and ACE) to access bis-diol frameworks of custom length and dihedral angle in an atom-economical manner. Indeed, the desired 90° tecton $\mathbf{3_{Me}}$ was synthesised on a 400 mg scale and the 180° tecton **4** up to 100 mg.

2.2 Boronic ester formation

Using 90° tecton $\mathbf{3_{Me}}$, an initial test reaction with 2.0 equiv. of phenyl boronic acid $\mathbf{15_H}$ was performed to assess boronic ester formation (Scheme 2). After reaction (microwave heating in EtOH, 5 min), a fine precipitate was isolated (63%) and analysis of the material using ^{1}H NMR spectroscopy indicated that the desired assembly ($\mathbf{[1 + 2]_H}$) had formed. The chemical shift of the resonance assigned to the terminal **CHOH** ($\delta = 4.32$ ppm, Scheme 2) of bis-diol $\mathbf{3_{Me}}$ was considerably different to that of the product containing a **CHOB** ($\delta = 5.18$ ppm, Scheme 2 and SI)

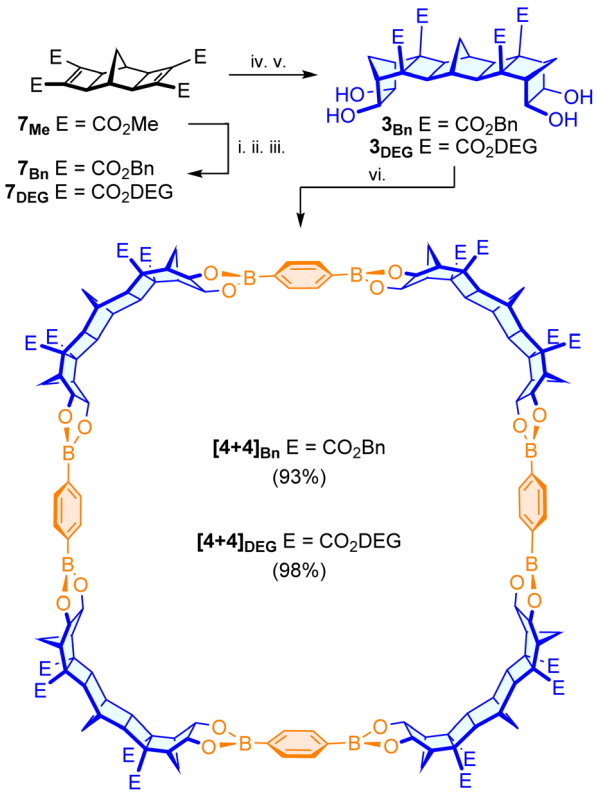

Scheme 3 Tuning of physical properties through ester modification. (i) KOH, H_2O : THF : MeOH (4 : 1 : 1), reflux, 24 h. (ii) $SOCl_2$, $CHCl_3$, reflux, 1.5 h. (iii) Benzyl alcohol or diethylene glycol monomethyl ether (4.5 eq.), $CHCl_3$, reflux, 2 h. (iv) CPD (8 eq.), DMF, RT, 7 days. (v) OsO_4 (1 mol%), NMO (3.0 eq.), acetone: H_2O, RT, 3 days. (vi) $CHCl_3$, 100 °C, 24 h.

and in the ^{1}H NMR spectrum the C**H**OH → C**H**OB change was diagnostic for complete boronic ester formation. Suitable single crystals of the assembly were grown from slow evaporation of a solution of the compound in hexane/$CHCl_3$, and the [1 + 2] structure confirmed by SC-XRD analysis (Scheme 2). Within the crystal structure, a dihedral angle between the boronic esters of 100° was established. Similarly, reaction of the 90° tecton $\mathbf{3_{Me}}$ with 2.0 equiv. of 4-fluorophenylboronic acid $\mathbf{15_F}$ gave the desired $\mathbf{[1 + 2]_F}$ boronic ester (49%, Scheme 2).

Given the expected stability of the norbornane boronic ester linkage, an investigation into the dynamic nature of the reaction was conducted. A 1 : 2 mixture of both $\mathbf{[1 + 2]_F}$ and free phenyl boronic acid $\mathbf{15_H}$ in (5 : 2) DMSO-d_6:$CDCl_3$ was prepared and monitored by ^{1}H and ^{19}F NMR spectroscopy (see SI for full details). Over 140 hours, resonances corresponding to the free fluorophenyl boronic acid $\mathbf{15_F}$ appeared, and resonances corresponding to the phenyl boronic acid $\mathbf{15_H}$ decreased. At equilibrium, the relative integrations of $\mathbf{15_H : 15_F}$ were approximately 1 : 1, suggesting little to no electronic effect on the lability of the boronic ester pair in this instance. Of interest, at no point were resonances corresponding to the free norbornane diol observed, indicating that the exchange of phenyl groups was likely proceeding through direct transesterification of the boronic esters. Given slow exchange occurred under mild conditions, the norbornane boronic esters appear to be suitably dynamic such that assembly processes are capable of error correction to form thermodynamic products.

2.3 Assembly: [4 + 4] macrocycles

The reaction of 90° tecton $\mathbf{3_{Me}}$ with benzene-1,4-diboronic acid **5** was performed using a method adapted from Mastalerz.[8] The two components were heated in chloroform overnight and following precipitation with hexanes and centrifugation, a fine white powder was isolated (99%). The powder was suitably soluble in chloroform, and ^{1}H NMR analysis indicated a similar change in the diagnostic C**H**OH resonances of the framework protons as those seen for the [1 + 2] assemblies (Scheme 2). In a single instance (using direct injection of a concentrated solution in $CHCl_3$) analysis by ESI-HRMS confirmed the synthesis was preceding to the desired [4 + 4] macrocycle, however the result was frustratingly irreproducible. This irreproducibility was attributed to the poor ionisation efficiency of the macrocycle and the low solubility of the assembly in polar solvents, necessitating the use of chloroform. Similarly, suitable crystals for SC-XRD analysis could not be grown. To validate the formation of the [4 + 4] macrocycle, molecular simulations were conducted. Hypothetical assemblies of [3 + 3], [4 + 4] and [5 + 5] macrocycles were generated, and atomic coordinates were optimised using density functional theory. Higher order assemblies (such as [6 + 6] or [7 + 7]) were presumed unrealistic due to the excessive ring strain required. The formation energy for the reaction producing water was computed to assess the relative energies of these assemblies (see SI). It was observed that the [4 + 4] macrocycle balances the strain and bond formation, leading to the lowest formation energy, whereas the [3 + 3] and [5 + 5] analogues are destabilised by ~20 kJ mol^{-1}.

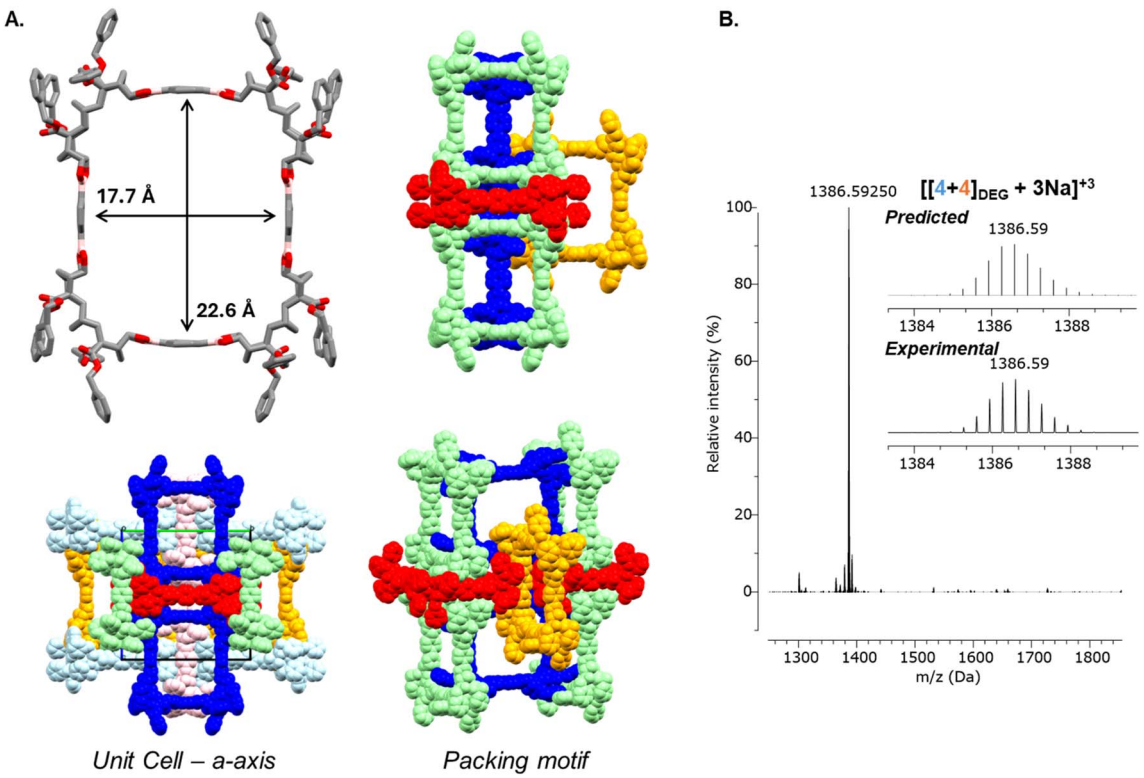

Fig. 2 (A) SC-XRD structure of macrocycle $[4 + 4]_{Bn}$, a portion of the unit cell is highlighted to emphasise the packing arrangement. (B) nESI-HRMS spectrum of macrocycle $[4 + 4]_{DEG}$.

These simulations highlight the [4 + 4] assembly is the expected, lowest energy, product.

It was envisaged that the physical properties of the assembly could be modulated by changing the methyl esters of the 90° tecton prior to reaction with the diboronic acid. To this end, the synthesis of analogues that contained benzyl esters (for enhanced crystallinity) and diethylene-glycol monomethyl ether (DEG) esters (for enhanced solubility) were pursued (Scheme 3). Hydrolysis of the methyl esters of tetraester $\mathbf{7_{Me}}$ and subsequent re-esterification (*via* acid chloride)[43] with the appropriate alcohol gave the desired tetraesters $\mathbf{7_{Bn}}$ and $\mathbf{7_{DEG}}$. The same sequence of twin-Diels–Alder cycloaddition and Upjohn dihydroxylation gave the desired ester modified bis-diols (see SI for details). Reaction of the tuned bis-diols $\mathbf{3_{Bn}}$ and $\mathbf{3_{DEG}}$ with benzene-1,4-diboronic acid **5** gave good yields of macrocyclic compounds (benzyl: 93%, DEG: 98%) that exhibited ^{1}H NMR spectra similar (other than the esters) to those of the macrocycle formed using bis-diol $\mathbf{3_{Me}}$ (see SI for details).

Pleasingly, the benzyl substituted boronic ester assembly $\mathbf{[4 + 4]_{Bn}}$ was amenable to crystallisation (see SI for full details) and high-quality cubic crystals were obtained by slow evaporation of a solution of $\mathbf{[4 + 4]_{Bn}}$ in DMSO/DCM/acetone. The crystal structure was solved in the body centred cubic space group *I*23. The large unit cell ($a = b = c = 33.945$ Å) and rapid desolvation (deterioration of the crystal) led to difficulty obtaining resolution beyond ~0.8 Å. Nevertheless, the X-ray structure was solved as the target, confirming that the synthesis was indeed proceeding to the expected [4 + 4] macrocycle. Interestingly, the macrocycle $\mathbf{[4 + 4]_{Bn}}$ appears as a rectangle in the crystal structure, seemingly as a result of crystal packing effects, with the shorter side of one rectangle fitting into the face (parallel to the longer side) of a second macrocycle (*i.e.* green macrocycles fitting into red macrocycles in Fig. 2A).

Due to its enhanced solubility, the DEG substituted macrocycle $\mathbf{[4 + 4]_{DEG}}$ was more readily analysed by nanoelectrospray ionisation high resolution mass spectrometry (nESI-HRMS). The most abundant ion (*m*/*z* 1386.5925) was in excellent agreement with both the predicted isotope pattern (Fig. 2B) and mass-to-charge of the triply sodiated [4 + 4] macrocycle (predicted *m*/*z* 1386.5922), confirming the selective synthesis of the [4 + 4] macrocycle. Other than the desired [4 + 4] macrocycles, no significant signals corresponding to other macrocycles or intermediates were present within the mass spectrum (Fig. 2B).

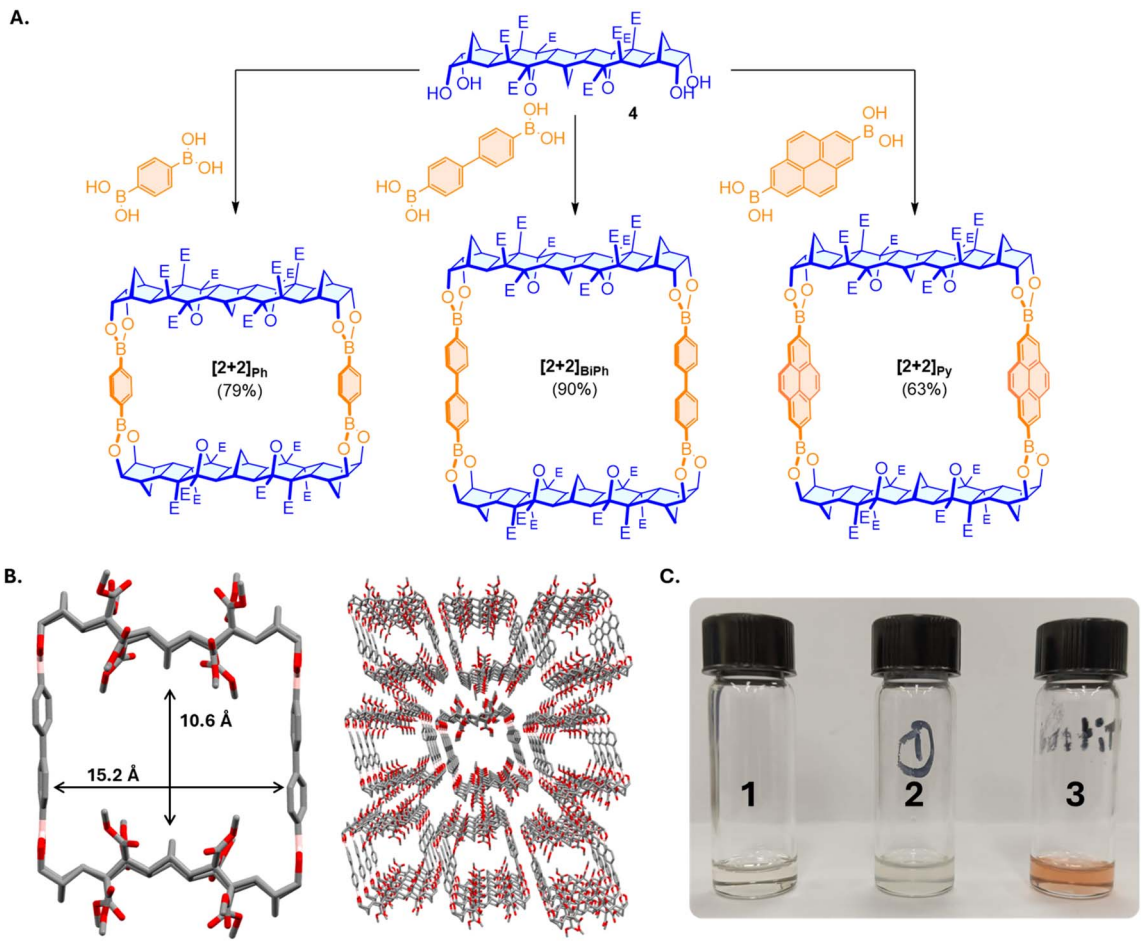

Scheme 4 (A) Synthesis of [2 + 2] macrocycles. $\mathbf{[2 + 2]_{Ph}}$ 79%, $\mathbf{[2 + 2]_{BiPh}}$ 90%, $\mathbf{[2 + 2]_{Py}}$ 63% (B) SC-XRD structure of $\mathbf{[2 + 2]_{BiPh}}$, the packing of the macrocycle is highlighted. (C) (1) Solution of methoxyethylamine-3,6-dinitro napthalimide in $CDCl_3$, (2) solution of macrocycle $\mathbf{[2 + 2]_{Py}}$ in $CDCl_3$, (3) solution of macrocycle $\mathbf{[2 + 2]_{Py}}$ with 20 equiv. of 3,6-dinitro-1,8-naphthalimide in $CDCl_3$.

Thus, the assembly of bis-diol $\mathbf{3_{Me}}$ (and its analogues) with benzene-1,4-diboronic acid exclusively and efficiently forms the desired [4 + 4] macrocycle, as confirmed by both crystallography and mass spectrometry.

2.4 Assembly: [2 + 2] macrocycles

Reaction of the longer 180° tecton **4** with benzene-1,4-diboronic acid **5** afforded a fine white powder in good yield (79%). The material was highly soluble in chloroform, and analysis by ^{1}H NMR spectroscopy once again indicated complete conversion to a boronic ester assembly using the diagnostic C**H**OB resonance. The structure was confirmed as the expected [2 + 2] macrocycle by means of HRMS analysis. Using the same protocol, macrocycles $\mathbf{[2+2]_{BiPh}}$ and $\mathbf{[2+2]_{Py}}$ were similarly accessed from 4,4′-biphenyldiboronic acid (90%) and pyrene-2,7-diboronic acid (63%) respectively.

To evaluate the overall structure of the architectures, single crystal XRD studies were conducted. Crystals of macrocycle $\mathbf{[2+2]_{BiPh}}$ were grown from slow diffusion of pentane into a solution of the macrocycle in chloroform. The packing arrangement involved macrocyclic units associating through offset π–π stacking[44] (see SI for details). The crystal structure presented a remarkable arrangement, with the macrocycles forming extended, potentially porous, channels through the crystal lattice. Macrocycle $\mathbf{[2+2]_{Py}}$ was thought to be suitable for inclusion of electron poor aromatic species and when a solution of 3,6-dinitro-1,8-naphthalimide was mixed with the macrocycle a vivid colour change was observed (Scheme 4, see SI for details).

2.5 Assembly: [3 + 2] cages

The condensation of bis-diol **4** with benzene-1,3,5-triboronic acid (3 : 2) gave a white powder in low yield (25%). Analysis of the isolated material by ^{1}H NMR spectroscopy revealed a remarkable spectrum, with four ester environments ($\delta = 3.61$, 3.77, 3.78, and 3.87 ppm) rather than the two expected for a C_3 symmetric species, and a noticeable "doubling" of several additional resonances assigned to the framework. The material was amenable to analysis by ESI-HRMS, and the mass obtained was in excellent agreement with the proposed [3 + 2] cage (see SI for details). While suitable single crystals could not be grown for structural analysis, AM1 molecular modelling (see SI for full details) provided insight into the possible structural arrangement and the poor yield. The likely cause of the desymmetrisation appeared to be steric interactions between the methyl ester substituents on either side of the cage aperture (Fig. 3B), leading to a twisting of the entire norbornane scaffold to minimise steric interactions. The twisting leads to a scenario where esters on one side of the framework sit slightly inside the central cavity (endohedral) and the esters of the other side are oriented exohedrally. The two environments give rise to the observed doubling of signals.

An extended cage compound $\mathbf{[3+2]_{TZ}}$ was efficiently accessed from reaction of 180° tecton **4** with triazine triphenyl triboronic acid (96%). Of interest ^{1}H NMR analysis of the extended cage provided a ^{1}H NMR spectrum with resonances in line with the expected C_3 and σ_v symmetric cage—again suggesting that steric issues were responsible for the lesser

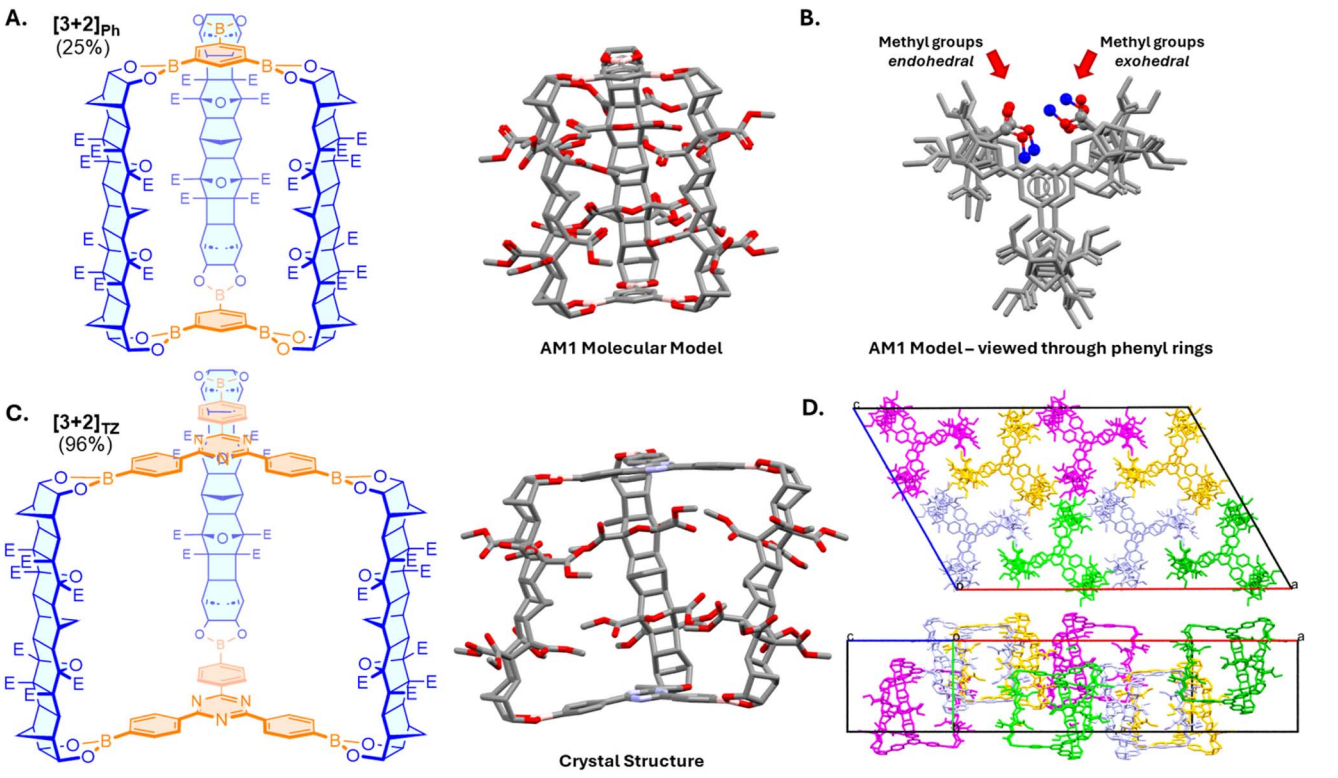

Fig. 3 (A) Cage $\mathbf{[3+2]_{Ph}}$ (25%) and molecular model. (B) Molecular model viewed along the phenyl rings highlighting the esters (methyl groups in blue). (C) Cage $\mathbf{[3+2]_{TZ}}$ (96%) and X-ray crystal structure. (D) Unit cell viewed along *b* axis (top) and *c** axis (bottom).

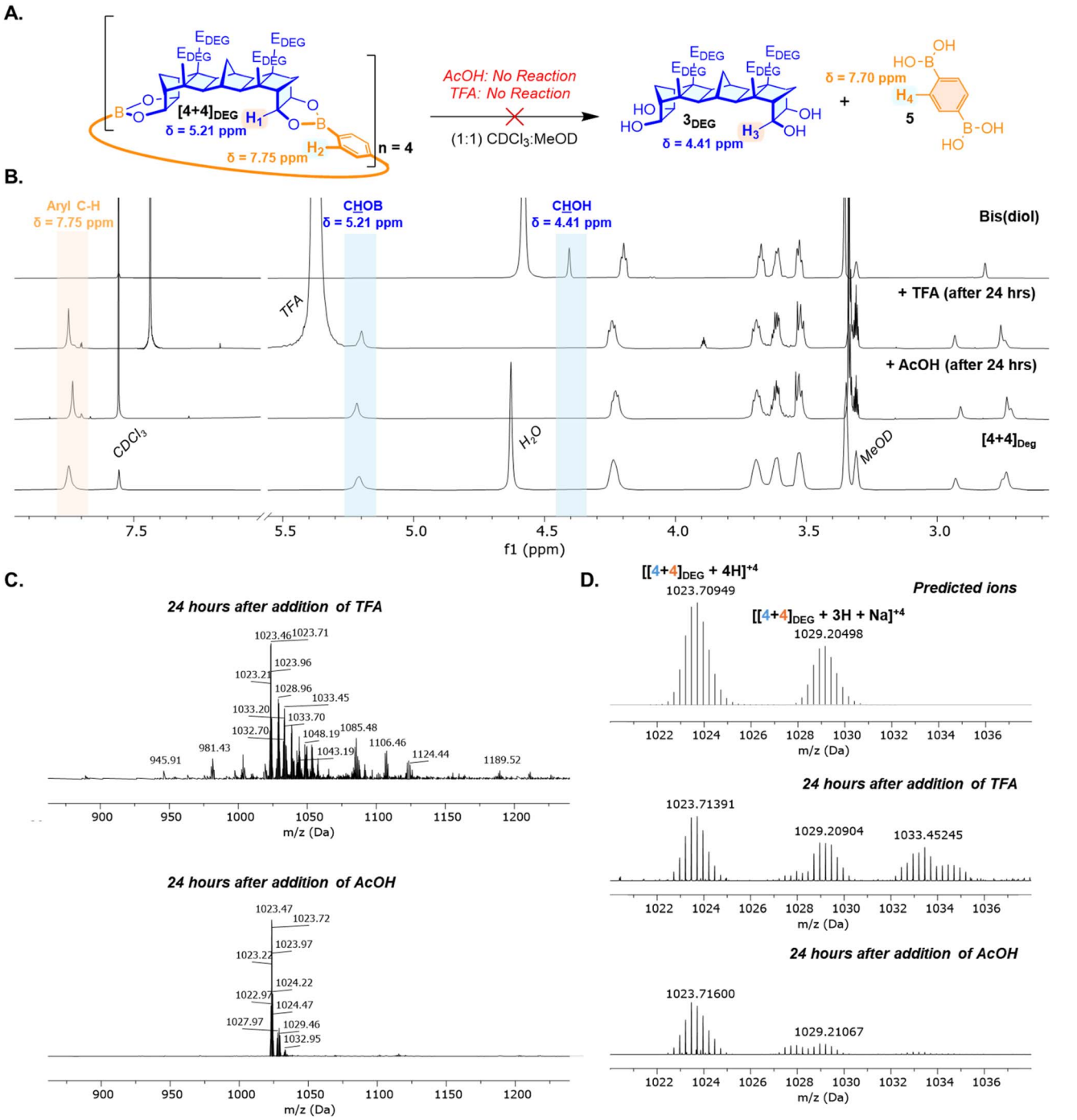

Fig. 4 Stability study of macrocycle $[4 + 4]_{DEG}$. (A) Expected resonances of hydrolysis products. (B) Stacked ^{1}H NMR spectra of macrocycle $[4 + 4]_{DEG}$ 24 hours after addition of AcOH or TFA. (C) Ion signals detected by nESI-HRMS of the samples after 24 hours, (D) highlights intact macrocycle.

symmetry of cage $[3 + 2]_{Ph}$. A ^{1}H diffusion spectrum of $[3 + 2]_{TZ}$ was obtained and a diffusion coefficient of 3.16×10^{-10} m^2 s^{-1} was derived. Using the Stokes–Einstein equation, the spherical radius of cage $[3 + 2]_{TZ}$ was calculated as 11.42 ± 0.12 Å, in excellent agreement with the expected size of the [3 + 2] molecular cage (see SI for full details).

Single crystals of cage $[3 + 2]_{TZ}$ were grown from slow diffusion of hexane into a solution of $[3 + 2]_{TZ}$ in chloroform. The needle crystals were amenable to analysis by SC-XRD. The overall packing of the cage along the *ac* plane relies on weak van der Waals forces between the windows of each cage (Fig. 3D), while along the *b* axis the triazine components of the cages stacked cofacially.

2.6 Hydrolytic stability

As a representative architecture of the norbornane boronic ester systems, the hydrolytic stability of macrocycle $[4 + 4]_{DEG}$ was

evaluated using a method adapted from Beuerle.[15] A solution of macrocycle $[\mathbf{4+4}]_{\mathbf{DEG}}$ was prepared in $CDCl_3$: MeOD (1 : 1) with acetic acid (final AcOH conc. 2.92 mM) and analysed using both ^{1}H NMR spectroscopy and nESI-HRMS. Over a 24-hour period no change in the sample was observed by ^{1}H NMR spectroscopy, and key resonances (Ar–H singlet $\delta = 7.75$ ppm and C**H**OB $\delta = 5.21$ ppm) remained present, indicating that the macrocycle was intact (Fig. 4B). Similarly, after 24 hours, analysis by nESI-HRMS clearly showed the presence of the intact macrocycle ($[\mathbf{4+4}]_{\mathbf{DEG}}$ (Fig. 4C, *m*/*z* 1023.47)).

Repeating the experiment with trifluoroacetic acid, a solution of the macrocycle $[\mathbf{4+4}]_{\mathbf{DEG}}$ was prepared in (1 : 1) $CDCl_3$: MeOD with trifluoroacetic acid (final TFA conc. 2.18 mM). After 24 hours, a very small resonance was noted in the ^{1}H NMR spectrum at $\delta = 7.70$ ppm that may suggest a degree of hydrolysis to a free boronic acid, however, the diagnostic C**H**OH resonance ($\delta = 4.41$ ppm) that would confirm disassembly was not apparent. Reassuringly, the key resonances of the macrocycle (phenyl singlet $\delta = 7.75$ ppm and C**H**OB $\delta = 5.21$ ppm) remained consistent, giving a strong indication that the macrocycle was intact. Analysis by means of nESI-HRMS was significantly complicated by the use of trifluoroacetic acid[45] and addition of sodium chloride was required to reduce analyte ion pairing and obtain a signal. As such, a significantly noisier spectrum was obtained that included multiple protonated/sodiated/hydrated species. Despite this, a signal coresponding to the $[[\mathbf{4+4}]_{\mathbf{DEG}} + 4\mathrm{H}]^{4+}$ ion was detected (*m*/*z* 1023.47) with the characteristic isotope pattern of the boronic ester assembly, giving further confirmation that the macrocycle was at least partially intact. Similarly an additional signal could be assigned to $[[\mathbf{4+4}]_{\mathbf{DEG}} + 3\mathrm{H} + \mathrm{Na}]^{4+}$ ion (Fig. 4, *m*/*z* 1029.20). Again, no signals corresponding to the expected hydrolysis products were noted (see SI for full details).

Similarly, using solely ^{1}H NMR spectroscopy, the hydrolytic stability of $[\mathbf{1+2}]_{\mathbf{Ph}}$, $[\mathbf{4+4}]_{\mathbf{Me}}$, $[\mathbf{2+2}]_{\mathbf{BiPh}}$ and $[\mathbf{3+2}]_{\mathbf{TZ}}$ cage were evaluated in the presence of both AcOH and TFA (in 35% to 50% MeOD/$CDCl_3$ subject to solubility, see SI for full details) and in each case no signals corresponding to hydrolysis products were observed after 24 hours. In comparison to the sterically protected [12 + 8] cage reported by Beuerle (Fig. 1),[15] the results here indicate that the norbornane boronic ester linkage also possesses remarkable hydrolytic stability without the need to functionalise the boronic acid component. Indeed, the stability to MeOH/TFA place this class of compounds as amongst the most hydrolytically stable boronic ester assemblies that have been reported.

3. Conclusion

The synthesis of two fused [*n*]polynorbornane based bis-diol tectons featuring differing lengths and 90° or 180° dihedral angles was successfully accomplished. Using a number of commercial di- and triboronic acids these tectons were efficiently assembled into a series of macrocyclic or cage-like boronic ester architectures. The hydrolytic stability of the new assemblies was evaluated, and the norbornane boronic ester linkage confirmed as an exceptionally stable connection for constructing larger assemblies. While existing catechol based linkages can be made stable by use of sterically hindered boronic acids, the use of norbornane diols provides a unique direction for the field of boronic ester assemblies whereby readily accessible fused [*n*]polynorbornane tectons (that can be tailored to varying geometries) can be partnered with a wide range of boronic acids to access a diverse range of architectures, including covalent organic frameworks, that are inherently stable to hydrolysis.

Author contributions

D. Coomber: conceptualization, formal analysis, investigation, methodology, writing – original draft preparation, writing – review & editing, O. Rusli: investigation, writing – review & editing, H. Sharma: investigation, H. E. Lee: investigation, J. D. Evans: investigation, resources, methodology, writing – review & editing, N. J. Rijs: resources, writing – review & editing, C. Hua: resources, supervision, writing – review & editing, F. Pfeffer: conceptualization, project administration, resources, supervision, writing – review & editing.

Conflicts of interest

There are no conflicts to declare.

Data availability

CCDC 2489231–2489235 contain the supplementary crystallographic data for this paper.[49a–e]

Supplementary information (SI): characterisation details (1H, 13C NMR spectra, crystallographic parameters) and full experimental procedures for the synthesis of all compounds are available in the supporting information. Additional hydrolysis experiments and X-ray crystallographic details are also available in the supporting information. See DOI: https://doi.org/10.1039/d5sc08385k.

Acknowledgements

D. C. would like to acknowledge funding support in the form of an Australian Government Research Training Program (RTP) Scholarship. Aspects of this research were funded by the Australian Government through the Australian Research Council (ARC) with both J. D. E. and N. J. R. being recipients of Australian Research Council Discovery Early Career Awards (DE220100163 and DE170100677 respectively). Award DE170100677 was used to fund MS instrumentation, consumables, MWAC time and a salary component. Aspects of this research were also supported by the Australian Government's National Collaborative Research Infrastructure Strategy (NCRIS), with access to computational resources provided by Pawsey Supercomputing Research Centre through the National Computational Merit Allocation Scheme. Both F. P. and D. C. would also like to acknowledge the Centre for Sustainable Bioproducts at Deakin University for additional funding. Phoenix HPC service (Adelaide University) is acknowledged for providing

high-performance computing resources. F. P. would also like to acknowledge a number of beneficial discussions related to this project that took place with generous members of the supramolecular chemistry community in both Germany and the United Kingdom. This research was undertaken in part using the MX1 (ref. 47) and MX2 (ref. 48) beamlines at the Australian Synchrotron, part of ANSTO, and made use of the Australian Cancer Research Foundation (ACRF) detector.

Notes and references

† The stability of boronic esters is based on many factors that include (i) the surrounding steric environment (ii) the ring size of the boronic ester, and (iii) electron density at the boron atom, a property influenced by both the nature of the aryl group (for phenylboronic acids) and also the electron donating propensity of the diol component.[46] While boronic esters derived from bicyclo[2.2.2]octane diols have not been explicitly tested for hydrolytic stability, they may also prove to be highly robust.

1 Y. H. Jin, Y. L. Zhu and W. Zhang, *Crystengcomm*, 2013, **15**, 1484–1499.
2 Z. Lin, T. J. Emge and R. Warmuth, *Chem.–Eur. J.*, 2011, **17**, 9395–9405.
3 S. P. Black, J. K. Sanders and A. R. Stefankiewicz, *Chem. Soc. Rev.*, 2014, **43**, 1861–1872.
4 W. Zhang and J. S. Moore, *Angew Chem. Int. Ed. Engl.*, 2006, **45**, 4416–4439.
5 Y. Jin, Q. Wang, P. Taynton and W. Zhang, *Acc. Chem. Res.*, 2014, **47**, 1575–1586.
6 R. C. Brachvogel and M. von Delius, *Eur. J. Org Chem.*, 2016, **2016**, 3662–3670.
7 K. Ono, K. Johmoto, N. Yasuda, H. Uekusa, S. Fujii, M. Kiguchi and N. Iwasawa, *J. Am. Chem. Soc.*, 2015, **137**, 7015–7018.
8 G. Zhang, O. Presly, F. White, I. M. Oppel and M. Mastalerz, *Angew Chem. Int. Ed. Engl.*, 2014, **53**, 1516–1520.
9 S. Ivanova, E. Koster, J. J. Holstein, N. Keller, G. H. Clever, T. Bein and F. Beuerle, *Angew Chem. Int. Ed. Engl.*, 2021, **60**, 17455–17463.
10 T. Uchikura, K. Ono, K. Takahashi and N. Iwasawa, *Angew Chem. Int. Ed. Engl.*, 2018, **57**, 2130–2133.
11 K. Ono, M. Niibe and N. Iwasawa, *Chem. Sci.*, 2019, **10**, 7627–7632.
12 M. K. Smith, A. R. Goldberg and B. H. Northrop, *Eur. J. Org Chem.*, 2015, **2015**, 2928–2941.
13 A. D. Chavez, B. J. Smith, M. K. Smith, P. A. Beaucage, B. H. Northrop and W. R. Dichtel, *Chem. Mater.*, 2016, **28**, 4884–4888.
14 S. Akine, D. Kusama, Y. Takatsuki and T. Nabeshima, *Tetrahedron Lett.*, 2015, **56**, 4880–4884.
15 P. H. Kirchner, L. Schramm, S. Ivanova, K. Shoyama, F. Wurthner and F. Beuerle, *J. Am. Chem. Soc.*, 2024, **146**, 5305–5315.
16 M. K. Smith, N. E. Powers-Riggs and B. H. Northrop, *Chem. Commun.*, 2013, **49**, 6167–6169.
17 V. Drogkaris and B. H. Northrop, *Org. Chem. Front.*, 2020, **7**, 1082–1094.
18 N. Nishimura and K. Kobayashi, *Angew Chem. Int. Ed. Engl.*, 2008, **47**, 6255–6258.
19 S. M. Elbert, N. I. Regenauer, D. Schindler, W. S. Zhang, F. Rominger, R. R. Schroder and M. Mastalerz, *Chem.–Eur. J.*, 2018, **24**, 11438–11443.
20 S. Klotzbach, T. Scherpf and F. Beuerle, *Chem. Commun.*, 2014, **50**, 12454–12457.
21 S. Klotzbach and F. Beuerle, *Angew Chem. Int. Ed. Engl.*, 2015, **54**, 10356–10360.
22 H. Sakurai, N. Iwasawa and K. Narasaka, *Bull. Chem. Soc. Jpn.*, 1996, **69**, 2585–2594.
23 N. Iwasawa and K. Ono, *Chem. Rec.*, 2022, **22**, e202100214.
24 S. Kasahara, H. Hayashi, T. Okumura, M. Matsumoto, M. Yamauchi, Y. Mizuhata, N. Aratani and H. Yamada, *Chempluschem*, 2025, **90**, e202500014.
25 R. Bernardini, A. Oliva, A. Paganelli, E. Menta, M. Grugni, S. De Munari and L. Goldoni, *Chem. Lett.*, 2009, **38**, 750–751.
26 C. D. Roy and H. C. Brown, *J. Organomet. Chem.*, 2007, **692**, 784–790.
27 C. D. Roy and H. C. Brown, *Monatsh. Chem.*, 2007, **138**, 879–887.
28 R. N. Warrener, I. G. Pitt and D. N. Butler, *J. Chem. Soc., Chem. Commun.*, 1983, 1340–1342.
29 R. N. Warrener, A. C. Schultz, D. N. Butler, S. Wang, I. B. Mahadevan and R. A. Russell, *Chem. Commun.*, 1997, 1023–1024.
30 R. Warrener, D. Margetic, R. Russell and E. Tiekink, *Synlett*, 1997, **2**, 3.
31 R. N. Warrener, *Eur. J. Org Chem.*, 2000, **2000**, 3363–3380.
32 R. C. Foitzik, A. J. Lowe and F. M. Pfeffer, *Tetrahedron Lett.*, 2009, **50**, 2583–2584.
33 M. D. Johnstone, A. J. Lowe, L. C. Henderson and F. M. Pfeffer, *Tetrahedron Lett.*, 2010, **51**, 5889–5891.
34 F. M. Pfeffer, T. Gunnlaugsson, P. Jensen and P. E. Kruger, *Org. Lett.*, 2005, **7**, 5357–5360.
35 A. J. Lowe and F. M. Pfeffer, *Org. Biomol. Chem.*, 2009, **7**, 4233–4240.
36 R. N. Robson, B. P. Hay and F. M. Pfeffer, *Eur. J. Org Chem.*, 2019, **2019**, 6720–6727.
37 M. D. Johnstone, M. Frank, G. H. Clever and F. M. Pfeffer, *Eur. J. Org Chem.*, 2013, **2013**, 5848–5853.
38 M. D. Johnstone, E. K. Schwarze, G. H. Clever and F. M. Pfeffer, *Chem.–Eur. J.*, 2015, **21**, 3948–3955.
39 W. Murrell, P. M. Usov, C. Hua and F. Pfeffer, *Chempluschem*, 2025, **90**, e202500065.
40 T. Mitsudo, K. Kokuryo, T. Shinsugi, Y. Nakagawa, Y. Watanabe and Y. Takegami, *J. Org. Chem.*, 1979, **44**, 4492–4495.
41 R. Nencka, M. Dejmek, H. Hřebabecký, M. Šála and M. Dračínský, *Synthesis*, 2011, 4077–4083.
42 T.-A. Mitsudo, K. Kokuryo and Y. Takegami, *J. Chem. Soc., Chem. Commun.*, 1976, **18**, 722–723.
43 D. Margetić, A. Briš, R. N. Warrener and D. N. Butler, *Tetrahedron*, 2013, **69**, 7403–7407.
44 C. Janiak, *J. Chem. Soc., Dalton Trans.*, 2000, 3885–3896.
45 C. C. Chan, M. S. Bolgar, D. Dalpathado and D. K. Lloyd, *Rapid Commun. Mass Spectrom.*, 2012, **26**, 1507–1514.

46 D. G. Hall, *Boronic Acids: Preparation and Applications in Organic Synthesis, Medicine and Materials*, Wiley, 2011.
47 N. P. Cowieson, D. Aragao, M. Clift, D. J. Ericsson, C. Gee, S. J. Harrop, N. Mudie, S. Panjikar, J. R. Price, A. Riboldi-Tunnicliffe, R. Williamson and T. Caradoc-Davies, *J. Synchrotron Radiat.*, 2015, **22**, 187–190.
48 D. Aragao, J. Aishima, H. Cherukuvada, R. Clarken, M. Clift, N. P. Cowieson, D. J. Ericsson, C. L. Gee, S. Macedo, N. Mudie, S. Panjikar, J. R. Price, A. Riboldi-Tunnicliffe, R. Rostan, R. Williamson and T. T. Caradoc-Davies, *J. Synchrotron Radiat.*, 2018, **25**, 885–891.
49 (*a*) CCDC 2489231: Experimental Crystal Structure Determination, 2026, DOI: 10.5517/ccdc.csd.cc2pk7s9; (*b*) CCDC 2489232: Experimental Crystal Structure Determination, 2026, DOI: 10.5517/ccdc.csd.cc2pk7tb; (*c*) CCDC 2489233: Experimental Crystal Structure Determination, 2026, DOI: 10.5517/ccdc.csd.cc2pk7vc; (*d*) CCDC 2489234: Experimental Crystal Structure Determination, 2026, DOI: 10.5517/ccdc.csd.cc2pk7wd; (*e*) CCDC 2489235: Experimental Crystal Structure Determination, 2026, DOI: 10.5517/ccdc.csd.cc2pk7xf.